Chinese Journal of
POLYMER SCIENCE

ARTICLE

https://doi.org/10.1007/s10118-018-2160-5
Chinese J. Polym. Sci. 2018, 36, 1361–1367

Antistatic PVC-graphene Composite through Plasticizer-mediated Exfoliation of Graphite

Zi-Bo Wei[a,b], Yang Zhao[a*], Chao Wang[a], Shigenori Kuga[a], Yong Huang[a], and Min Wu[a*]

[a] *Technical Institute of Physics and Chemistry, Chinese Academy of Sciences, Beijing 100190, China*
[b] *University of Chinese Academy of Sciences, Beijing 100049, China*

Abstract Multilayer graphene was prepared by mechanical exfoliation of natural graphite with dioctyl phthalate (DOP) as milling medium without solvent. The obtained mixture could be directly mixed with poly(vinyl chloride) (PVC) for melt-forming, with DOP acting as plasticizer and graphene acting as conductive filler for antistatic performance. The composite showed surface resistance of 2.5×10^6 Ω/□ at 1 wt% carbon additive, significantly lower than approx. 7 wt% of raw graphite required for achieving the same level. This value is low enough for practical antistatic criterion of 3×10^8 Ω/□. The effect of filler addition on mechanical performance was minimal, or even beneficial for the milled carbon in contrast to the case of raw graphite.

Keywords Antistatic composite; Poly(vinyl chloride); Graphene; Mechanical exfoliation; Electrical property

Citation: Wei, Z. B.; Zhao, Y.; Wang, C.; Kuga, S.; Huang, Y.; Wu, M. Antistatic PVC-graphene Composite through Plasticizer-mediated Exfoliation of Graphite. Chinese J. Polym. Sci. 2018, 36(12), 1361–1367.

INTRODUCTION

Poly(vinyl chloride) (PVC) is a major commodity polymer used for insulator, flooring and construction pipes based on its chemical-, flame- and corrosion-resistance[1]. However, insulation property of PVC makes it prone to electrostatic charging-up, which can cause sparks leading to fire. In circumstances like chemical plants, gas stations and coal mines, antistatic-modified PVC products are important for ensuring safety[2]. Many methods have been proposed to improve the antistatic property of PVC products, and addition of conductive filler is known to be effective. For example, graphite[3], carbon black[4] and carbon fiber[5] have been used to enhance conductivity of PVC composites. However a high loading, generally up to 30 wt%, of these carbon materials is needed to meet the performance requirements. Such high loadings can sacrifice the mechanical properties and process performance of the material. Similar to conductive fillers, nanoscale carbon materials such as graphite powder[6], carbon nanotube (CNT)[7, 8] and graphene[9, 10] aroused great interests. The graphene-PVC composites reported so far were prepared by *in situ* polymerization or addition of graphene[1, 11, 12], but the dispersion of graphene in the matrix is generally difficult.

Ball milling is an effective way for exfoliating graphite into graphene/multilayer graphene[13–15]. There are two modes in ball mill processing: dry and wet. Dry milling of neat graphite can realize quick exfoliation, but accompanies destruction of the graphene sheet structure leading to amorphization and thus loss of electric conductivity[16]. In contrast, wet milling, *i.e.* milling with an inert liquid, gives milder ball impacts, better protecting the graphene structure[15, 17]. Difficulty in wet milling is the use of large amounts of solvent and its subsequent removal. Thus, finding an effective method of wet milling with no necessity to remove the solvent is very important.

We here propose the use of dioctyl phthalate (DOP) as graphite milling medium. DOP is a widely used plasticizer of commodity plastics including PVC. Therefore, if it is effective as medium for graphite milling, this approach can be useful for impregnating PVC with graphene. Besides the anti-static effect, influence of graphene addition on the mechanical properties is also of interest. We present below the results of the assessment together with microscopic observation of filler-matrix interface to confirm good compatibility.

EXPERIMENTAL

Materials

Poly(vinyl chloride) (PVC SG-5) in powder form was supplied by Inner Mongolia Junzheng Energy & Chemical Industry (China); calcium/zinc compound stabilizer was supplied by Tiantang Auxiliaries Chemical (China); dioctyl phthalate (DOP) was supplied by Macklin Biochemical (China) and used as received; graphite flake (150 μm) was obtained from Qingdao Tianheda Graphite (China).

Preparation of the Graphene-PVC Composite

Typically, 4 g of graphite flake and 30 g of DOP were loaded

* Corresponding authors: E-mail yzhao@mail.ipc.ac.cn (Y.Z.)
E-mail wumin@mail.ipc.ac.cn (M.W.)

Received March 23, 2018; Accepted May 19, 2018; Published online June 14, 2018

to a 350-mL agate pot containing 300 g of 1.0 cm zirconia balls. The pot was operated by a planetary mill (QM3SP4, Nanjing University Instrument Plant) at 540 r/min for 24 h. The resulting suspension was mixed with 70 g of PVC powder and 3 g of stabilizer in a high-speed dispersion machine (DFY-500, Wenzhou Dingli Medical Equipment Co.). The mixture was injection-molded by a Haake MiniJet Pro. The injection conditions were 175 °C and 70 MPa, then holding pressure for 5 s. The square specimens (100 mm × 100 mm × 2 mm) were molded by a hot press at 170 °C (Fig. 1). The graphite-PVC composite for comparison was prepared by the same procedure except ball-milling.

Characterization

Microscopic structure was examined by scanning electron microscopy (Hitachi S-4800, operated at 10 kV), transmission electron microscopy (JEOL E-2100) and atomic force microscopy (Bruker Multimode 8). The graphene/graphite samples for SEM were prepared by the method of dispersing graphene/graphite in ethanol, and adding dropwise on sticky rubber substrate. The samples for TEM were prepared by adding the 0.05 wt% graphene/graphite ethanol dispersion on copper grid. Raman spectroscopy was conducted by a 532 nm laser with an Raman spectrometer (inVia-Reflex) equipped with an air cooled CCD detector.

The electrical resistivity of the composites was measured by megohmmeter (ACL Model 800). Tensile test was done by a universal testing machine (Instron 5966) with crosshead speed of 5 mm/min. At least five samples were tested for each composition. The standard for tensile tests is GB/T 1040-2006.

RESULTS AND DISCUSSION

Characterization of Exfoliated Graphene

The starting graphite and the ball-milled graphene were dispersed in ethanol and irradiated by laser beam as shown in Fig. 2. The graphite particles settled down in less than 1 h and supernatant was nearly transparent. In contrast, the ball-milled product (Fig. 2b) had a small amount of precipitate and the supernatant showed clear Tyndall scattering, indicating colloidal dispersion of graphene[18].

The exfoliated graphene was examined by transmission electron microscopy as shown in Fig. 3. Figs. 3(a) and 3(b) show that the graphene had thin lamellar structure with lateral dimensions of several micrometers. Two electron diffraction (ED) patterns taken from the positions of the white spot (Fig. 3c) and black spot (Fig. 3d) showed the typical hexagonal symmetry of graphite or graphene[19, 20], demonstrating that the obtained graphene or graphite sheets had high crystallinity. Diffraction intensities taken along the 1–210 to −2110 axis for the patterns in Figs. 3(c) and 3(d) are respectively shown in Figs. 3(e) and 3(f). $I_{\{1100\}}/I_{\{2110\}} > 1$ in Fig. 3(e) demonstrates that the edge of graphene sheets possessed good crystallinity and single layer[21], and $I_{\{1100\}}/I_{\{2110\}} < 1$ in Fig. 3(f) indicates the multilayer graphene structure[22].

Fig. 4 shows the typical tapping-mode AFM image of the graphene flakes deposited on mica substrate. The lateral dimension is around 200 nm. The topographic profile corresponding to the mark lines blue and red crosses shows the thickness of graphene sheet to be approx. 3.3 nm,

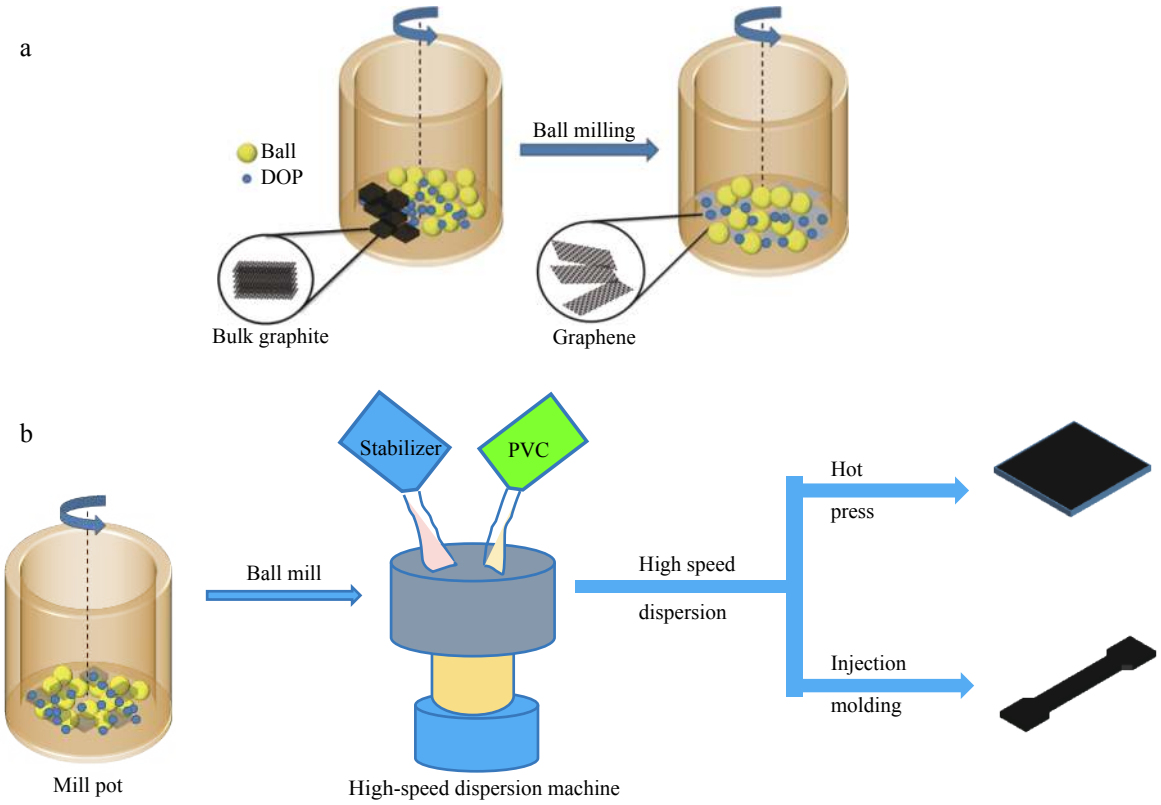

Fig. 1 Schematic diagrams of (a) preparing graphene by ball milling with DOP, and (b) preparing graphene-PVC composite.

https://doi.org/10.1007/s10118-018-2160-5

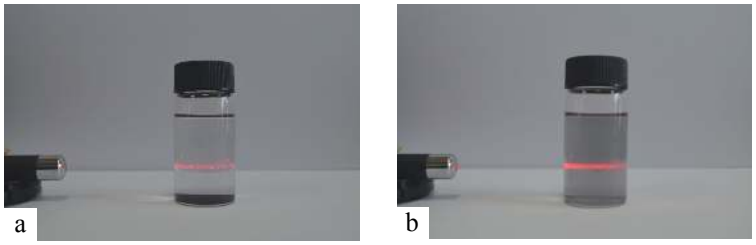

Fig. 2 (a) Graphite and (b) ball-milled products dispersed in ethanol, irradiated by a laser beam after 1 h standing

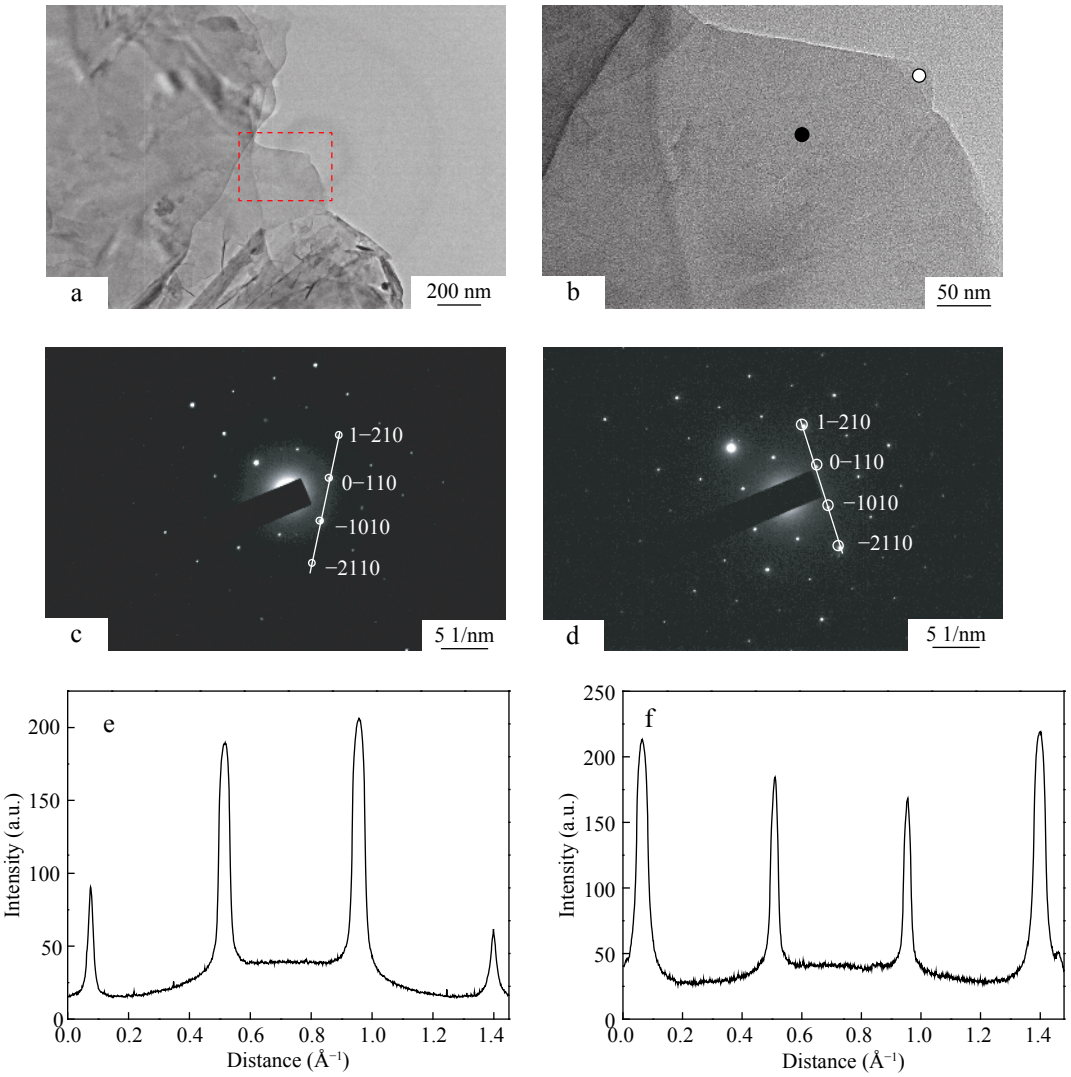

Fig. 3 (a) TEM images of graphene sheet obtained by ball milling and (b) high resolution image of marked region in (a); (c) Electron diffraction patterns taken from the positions of white spot in (b), and (d) of the black spot in (b); (e, f) Diffraction intensity taken along the 1–210 to −2110 axis for the patterns in (c) and (d), respectively

indicating multilayers of about 10 single sheets.

According to X-ray photoelectron spectroscopy (XPS) measurements, the surface of the as-prepared graphene is similar to those of the raw material graphite (Fig. 5), indicating that only the graphite surface was protected by DOP[23]. The carbon percentage of the graphene and graphite was calculated, and the results had no significant differences, indicating that there existed neither in-plane defect nor functionalization in the obtained graphene products[24].

Fig. 6(a) shows the Raman spectra of the bulk graphite and graphene sheets. Three important peaks are G at ~1580 cm^{-1}, D at ~1350 cm^{-1} and 2D at ~2700 cm^{-1}[25]. The G peak is due to the bond stretching of all pairs of sp^2 atoms in both rings and chains; the D peak is due to breathing modes of sp^2 atoms in rings[26, 27]. Fig. 6(a) compares the Raman spectra of graphene and graphite. It shows a notable

https://doi.org/10.1007/s10118-018-2160-5

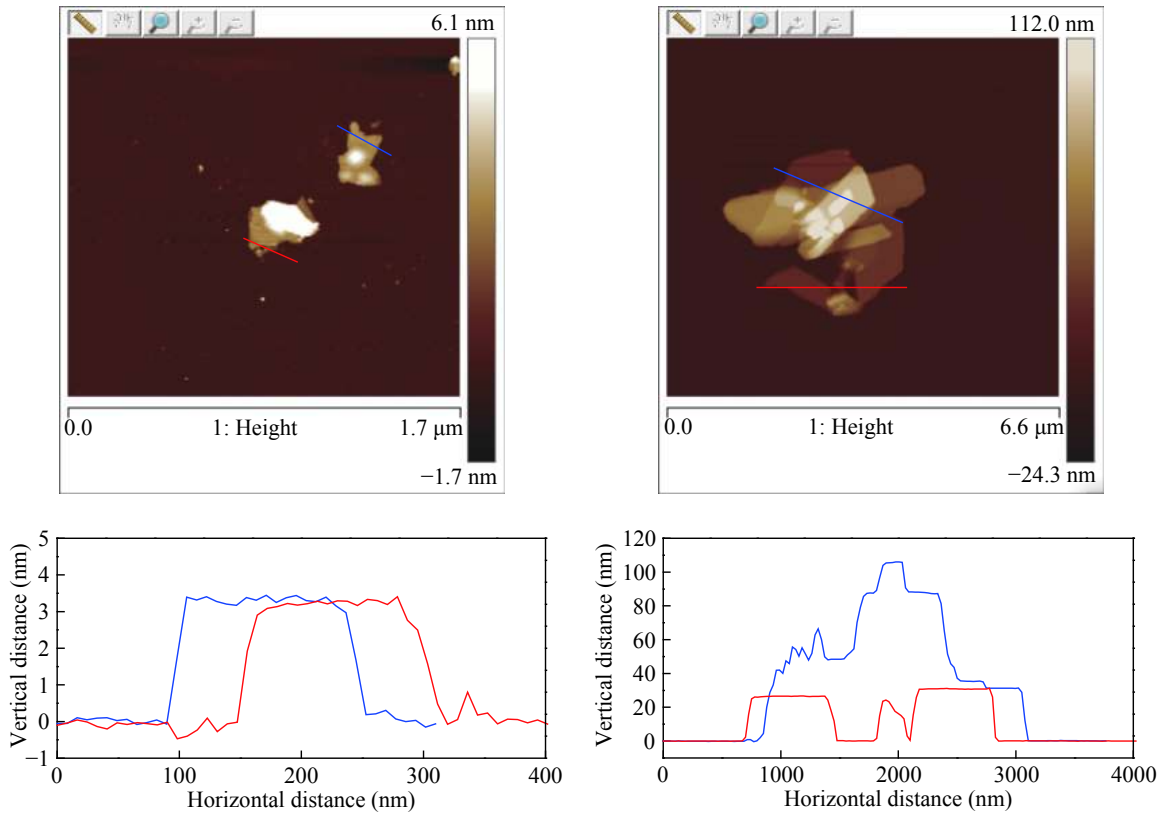

Fig. 4 AFM images of multilayer graphene sheets obtained by mechanical exfoliation. Typical thickness ranges from 3 nm to 30 nm.

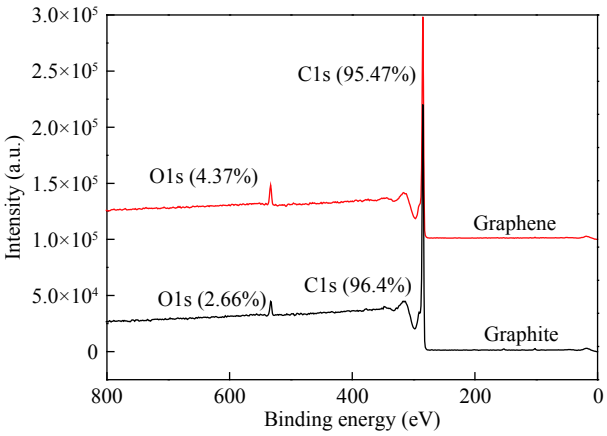

Fig. 5 XPS spectrum of graphite and exfoliated graphene

change in the shape of 2D peak between the two. Fig. 6(b) shows that 2D peak of graphite consists of two components named $2D_1$ and $2D_2$[25, 28] while graphene has a single 2D peak. The shape of this 2D peak is not sharp as that of single-layer graphene[29], but similar to the peak of few layer-graphene[29, 30]. Similar results have been reported for few-layer graphene prepared by mechanical exfoliation[26, 31].

Antistatic Properties of Graphene-PVC Composites

General criterion for antistatic performance is surface resistivity lower than 3×10^8 Ω/□ for PVC[1]. Fig. 7 shows the effects of graphite and graphene on electrical resistivity of the corresponding PVC composites. The resistivity of neat PVC is about 10^{16} Ω·cm[32]. Loading of graphene/graphite naturally reduces resistivity drastically, but the effectiveness differs greatly for the two. Loading level to reach the criterion is approx. 0.8% for graphene, while it is approx. 7% for graphite. This difference obviously results from the drastic increase in the particle population by exfoliation, leading to reduced percolation threshold for graphene.

Mechanical Properties of Graphene-PVC Composite

In general, use of inorganic fillers causes increase in stiffness and decrease in tensile strength. Fig. 8 shows tensile behavior of the composites. Both graphite and graphene additions cause an increase in Young's modulus, but there are remarkable differences between the two. The modulus of graphite composites stayed at nearly the same up to 7% loading, and from there rose steeply with loading up to 20%. In contrast, the modulus of graphene composite rose steadily up to 4% loading to give increase from 25 MPa to 33 MPa. More remarkable difference is seen in tensile strength. While graphite loading caused significant decrease from 15 MPa to 10 MPa, graphene loading gave nearly constant levels of approx. 15 MPa. Correspondingly, the change in elongation at break was more significant for graphite. One must note the difference in loading level scales in the comparisons, but it is clear that at the loading levels to give necessary reduction in resistivity, graphene loading has the minimal detrimental effect on the tensile properties.

Fig. 9 shows SEM images of the original graphite particles

https://doi.org/10.1007/s10118-018-2160-5

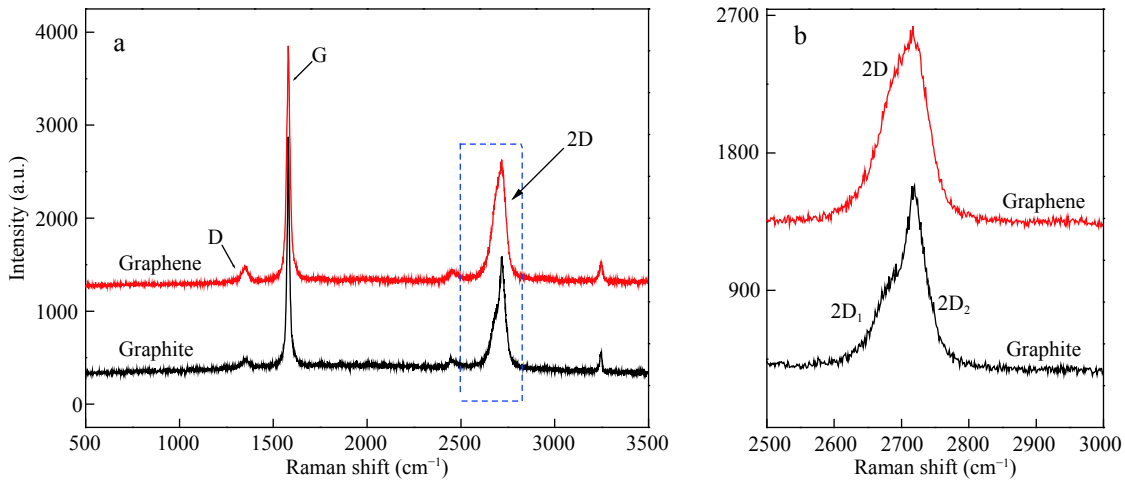

Fig. 6 (a) Comparison of the Raman spectra for graphene and graphite measured at 532 nm; (b) Comparison of the 2D peaks in graphene and graphite

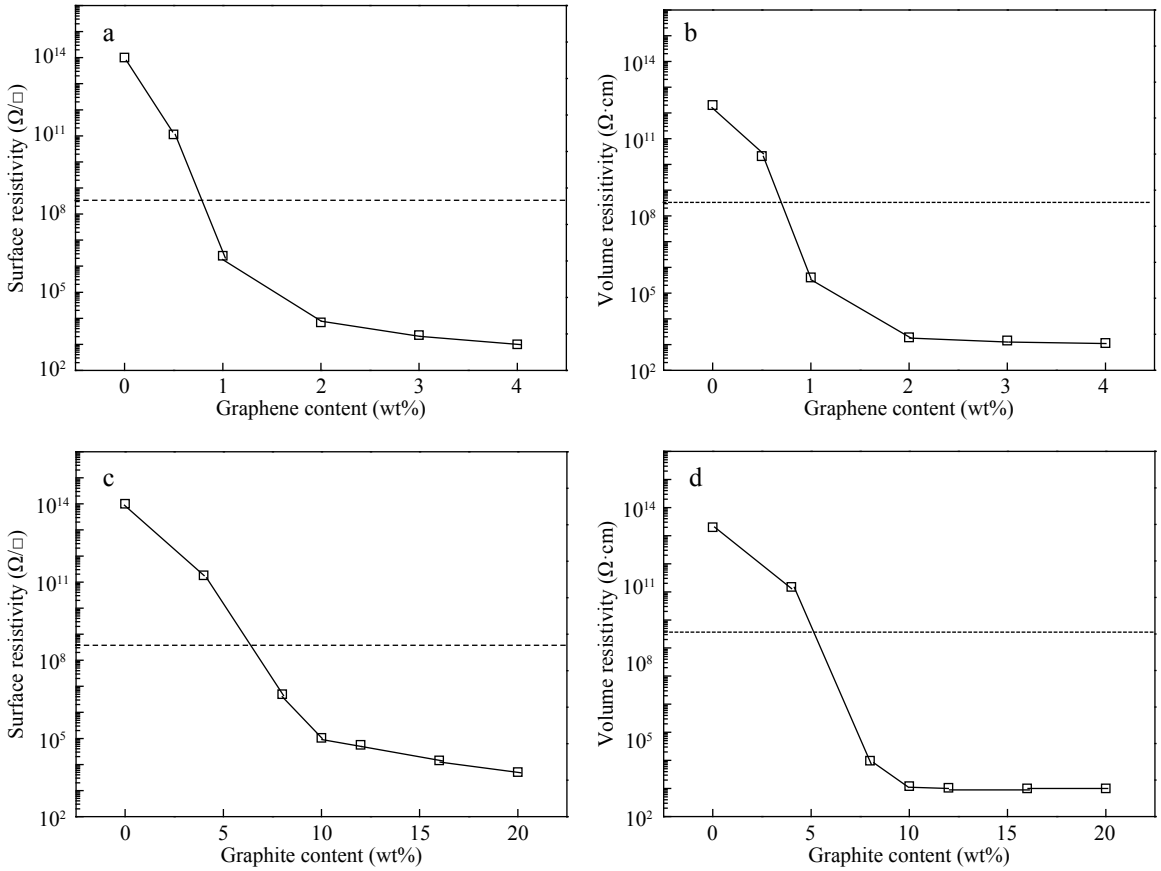

Fig. 7 (a, c) Surface and (b, d) volume resistivity of PVC composites: (a, b) graphene, (c, d) graphite. Note the difference in ordinate scales. Horizontal dotted lines show criterion for antistatic performance.

and the exfoliated graphene by DOP milling. The latter was extensively comminuted, and densely stack-aggregated on the substrate. Fig. 10 shows the tensile-fractured section of graphite- and graphene-PVC composites. Comparison of low-magnification images (Figs. 10a and 10b) indicates that graphene particles were much finer and more homogeneously dispersed in the matrix, and only the high-magnification image (Fig. 10c) shows protruding graphene particles clearly. In contrast, the graphite composite showed more rugged cross sections with large graphite flakes protruding to make cavities (Fig. 10a). Fig. 10(d) presents cross section of the graphene composite made by bending fracture, which exhibits features similar to Fig. 10(b). The EDS elemental mapping of C and Cl for this specimen (Figs. 10e and 10f) shows highly homogeneous distribution of graphene in the matrix. These microscopic features correspond well with the superior electric and mechanical performances described above.

https://doi.org/10.1007/s10118-018-2160-5

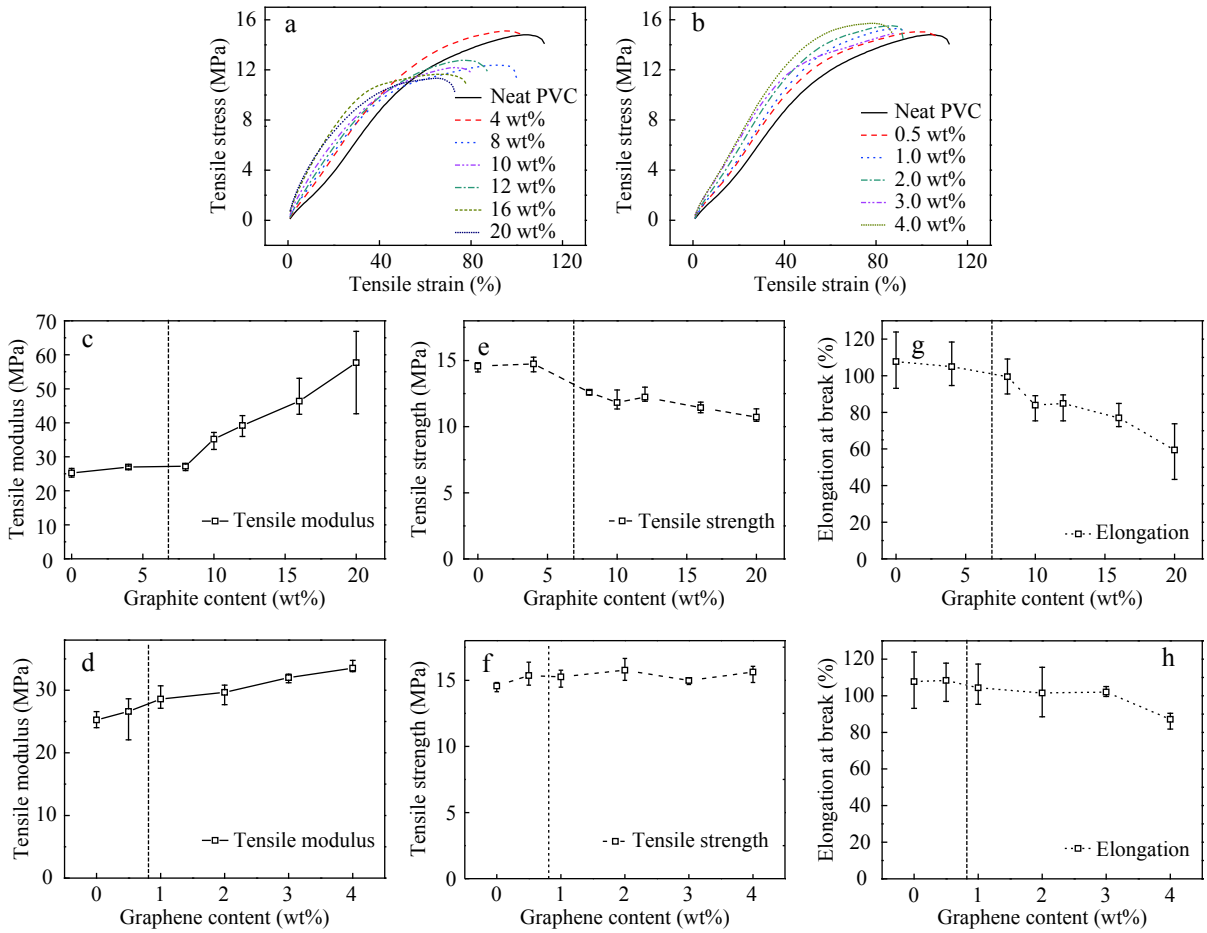

Fig. 8 Tensile properties of graphite/graphene-PVC composites: (a, c, e, g) graphite, (b, d, f, h) graphene. Note the difference in ordinate scale. Vertical dotted lines show the minimum loading level for antistatic performance.

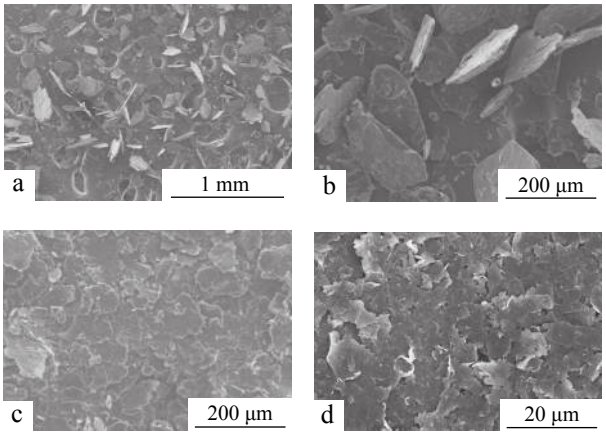

Fig. 9 SEM images of (a, b) original graphite dispersed on sticky rubber substrate, and (c, d) multilayer graphene, surface of deposited layer

CONCLUSIONS

Our examination of ball milling graphite with DOP, a representative plasticizer, showed that the product was multilayer graphene sheets maintaining high crystallinity, and that they could be readily loaded to PVC to form slightly conductive, anti-static composite. The loading level

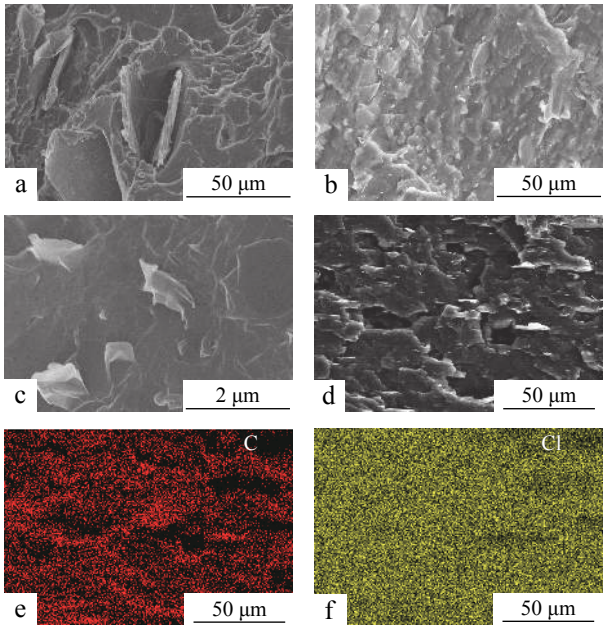

Fig. 10 SEM images of the tensile-fractured surface of composites: (a) graphite-PVC composite, (b) graphene-PVC composite, and (c) high magnified image of (b); (d) SEM image of bend-fractured surface of graphene-PVC composite; (e, f) EDS element mapping of C and Cl, respectively

https://doi.org/10.1007/s10118-018-2160-5

necessary for surface resistivity of 3×10^8 Ω/□ was approx. 0.8 wt%, and detrimental effect to mechanical performances was minimal. This method of plasticizer-mediated milling of graphite for anti-static loading would be practically useful for plastic materials at large scale.

ACKNOWLEDGMENTS

This work was financially supported by the National Natural Science Foundation of China (Nos. 51472253 and 51772306).

REFERENCES

1 Wang, H.; Xie, G.; Fang, M.; Ying, Z.; Tong, Y.; Zeng, Y. Electrical and mechanical properties of antistatic PVC films containing multi-layer graphene. Compos. Part B 2015, 79, 444−450.
2 Moulay, S. Chemical modification of poly(vinyl chloride)-Still on the run. Prog. Polym. Sci. 2010, 35(3), 303−331.
3 Murthy, K.; Ramkumar, K.; Satyam, M. Electrical properties of PVC-graphite thick films. J. Mater. Sci. Lett. 1984, 3(9), 813−816.
4 Noguchi, T.; Nagai, T.; Seto, J. E. Melt viscosity and electrical conductivity of carbon black PVC composite. J. Appl. Polym. Sci. 1986, 31(6), 1913−1924.
5 Wang, G. Q.; Zeng, P. Electrical conductivity of poly(vinyl chloride) plastisol short carbon filter composite. Polym. Eng. Sci. 1997, 37(1), 96−100.
6 Wu, X.; Qiu, J.; Liu, P., Sakai, E. Preparation and characterization of polyamide composites with modified graphite powders. J. Polym. Res. 2013, 20(11), 284.
7 Yazdani, H.; Smith, B. E.; Hatami, K. Multi-walled carbon nanotube-filled polyvinyl chloride composites: Influence of processing method on dispersion quality, electrical conductivity and mechanical properties. Compos. Part A 2016, 82, 65−77.
8 Zhang, M.; Zhang, C.; Du, Z.; Li, H.; Zou, W. Preparation of antistatic polystyrene superfine powder with polystyrene modified carbon nanotubes as antistatic agent. Compos. Sci. Technol. 2017, 138, 1−7.
9 Lei, L.; Qiu, J.; Sakai, E. Preparing conductive poly(lactic acid) (PLA) with poly(methyl methacrylate) (PMMA) functionalized graphene (PFG) by admicellar polymerization. Chem. Eng. J. 2012, 209, 20−27.
10 Wang, H.; Xie, G. Y.; Ying, Z.; Tong, Y.; Zeng, Y. Enhanced mechanical properties of multi-layer graphene filled poly(vinyl chloride) composite films. J. Mater. Sci. Technol. 2015, 31(4), 340−344.
11 Wang, H.; Zhang, H.; Zhao, W.; Zhang, W.; Chen, G. Preparation of polymer/oriented graphite nanosheet composite by electric field-inducement. Compos. Sci. Technol. 2008, 68(1), 238−243.
12 Li, J.; Kim, J. K. Percolation threshold of conducting polymer composites containing 3D randomly distributed graphite nanoplatelets. Compos. Sci. Technol. 2007, 67(10), 2114−2120.
13 Milev, A.; Wilson, M.; Kannangara, G. S. K.; Tran, N. X-ray diffraction line profile analysis of nanocrystalline graphite. Materials Chem. & Phys. 2008, 111(2-3), 346−350.
14 Montone, A.; Grbovic, J.; Bassetti, A.; Mirenghi, L.; Rotolo, P.; Bonetti, E. Microstructure, surface properties and hydrating behaviour of Mg-C composites prepared by ball milling with benzene. Int. J. Hydrogen Energ. 2006, 31(14), 2088−2096.
15 Yao, Y. G.; Lin, Z. Y.; Li, Z.; Song, X. J.; Moon, K. S.; Wong, C. P. Large-scale production of two-dimensional nanosheets. J. Mater. Chem. 2012, 22(27), 13494−13499.
16 Welham, N. J.; Berbenni, V.; Chapman, P. G. Effect of extended ball milling on graphite. J. Alloy. Compd. 2003, 349(1-2), 255−263.
17 Antisari, M. V.; Montone, A.; Jovic, N.; Piscopiello, E.; Alvani, C.; Pilloni, L. Low energy pure shear milling: A method for the preparation of graphite nano-sheets. Scripta. Mater. 2006, 55(11), 1047−1050.
18 Zhang, K.; Zhang, X.; Li, H.; Xing, X.; Jin, L.; Cao, Q. Direct exfoliation of graphite into graphene in aqueous solution using a novel surfactant obtained from used engine oil. J. Mater. Sci. 2017, 53(4), 2484−2496.
19 Meyer, J. C.; Geim, A. K.; Katsnelson, M. I.; Novoselov, K. S.; Booth, T. J.; Roth, S. The structure of suspended graphene sheets. Nature 2007, 446(7131), 60−63.
20 Meyer, J. C.; Geim, A. K.; Katsnelson, M. I.; Novoselov, K. S.; Obergfell, D.; Roth, S. On the roughness of single- and bi-layer graphene membranes. Solid State Commun. 2007, 143(1-2), 101−109.
21 Horiuchi, S.; Gotou, T.; Fujiwara, M.; Sotoaka, R.; Hirata, M.; Kimoto, K. Carbon nanofilm with a new structure and property. Japanese J. Appl. Phys. 2003, 42(Part 2, No.9A/B), L1073−L1076.
22 Hernandez, Y.; Nicolosi, V.; Lotya, M.; Blighe, F. M.; Sun, Z.; De, S. High-yield production of graphene by liquid-phase exfoliation of graphite. Nat. Nanotech. 2008, 3(9), 563−568.
23 Hansora, D. P.; Shimpi, N. G.; Mishra, S. Graphite to graphene *via* graphene oxide: an overview on synthesis, properties, and applications. JOM 2015, 67(12), 2855−2868.
24 Vadukumpully, S.; Paul, J.; Valiyaveettil, S. Cationic surfactant mediated exfoliation of graphite into graphene flakes. Carbon 2009, 47(14), 3288−3294.
25 Vidano, R. P.; Fischbach, D. B.; Willis, L. J.; Loehr, T. M. Observation of raman band shifting with excitation wavelength for carbons and graphites. Solid State Commun. 1981, 39(2), 341−344.
26 Graf, D.; Molitor, F.; Ensslin, K.; Stampfer, C.; Jungen, A.; Hierold, C. Spatially resolved raman spectroscopy of single- and few-layer graphene. Nano Lett. 2007, 7(2), 238−242.
27 Castiglioni, C.; Negri, F.; Rigolio, M.; Zerbi, G. Raman activation in disordered graphites of the A1' symmetry forbidden k≠0 phonon: The origin of the D line. J. Chem. Phys. 2001, 115(8), 3769−3778.
28 Nemanich, R. J.; Solin, S. A. 1st-order and 2nd-order Raman-scattering from finite-size crystals of graphite. Phys. Rev. B 1979, 20(2), 392−401.
29 Ferrari, A. C. Raman spectroscopy of graphene and graphite: Disorder, electron-phonon coupling, doping and nonadiabatic effects. Solid State Commun. 2007, 143(1-2), 47−57.
30 Ferrari, A. C.; Meyer, J. C.; Scardaci, V.; Casiraghi, C.; Lazzeri, M.; Mauri, F. Raman spectrum of graphene and graphene layers. Phys. Rev. Lett. 2006, 97(18), 187401.
31 Gupta, A.; Chen, G.; Joshi, P.; Tadigadapa, S.; Eklund, P. C. Raman scattering from high-frequency phonons in supported n-graphene layer films. Nano Lett. 2006, 6(12), 2667−2673.
32 Menges, G. Werkstoffkunde Kunststoffe, Carl Hanser Ver-lag München Wien, 3, Auflage, 1990, p 217-218.

https://doi.org/10.1007/s10118-018-2160-5